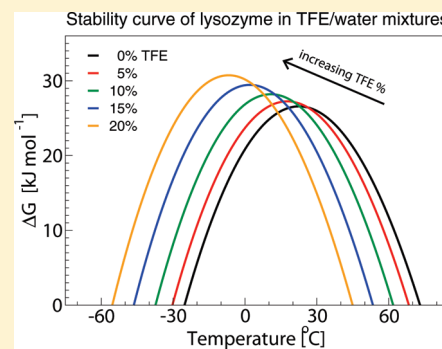


# Existence of Metastable Intermediate Lysozyme Conformation Highlights the Role of Alcohols in Altering Protein Stability

Michele D'Amico,<sup>†,§</sup> Samuele Raccosta,<sup>†,‡</sup> Marco Cannas,<sup>‡</sup> Vincenzo Martorana,<sup>†</sup> and Mauro Manno<sup>\*,†</sup><sup>†</sup>Institute of Biophysics at Palermo (IBF), National Research Council of Italy (CNR), via U. La Malfa 153, I-90146 Palermo, Italy<sup>‡</sup>Dipartimento di Fisica, Università di Palermo, via Archirafi 36, I-90123 Palermo, Italy**S Supporting Information**

**ABSTRACT:** Alcohols have a manifold effect on the conformational and thermodynamic stability of native proteins. Here, we study the effect of moderate concentrations of trifluoroethanol (TFE) on the thermal stability of hen egg-white lysozyme (HEWL), by far-UV circular dichroism and by steady-state and time-resolved photoluminescence of intrinsic tryptophans. Our results highlight that TFE affects lysozyme stability by preferential solvation of the protein molecule. Furthermore, we discovered the existence at 20% TFE of an equilibrium partially folded state of lysozyme, intermediate between the native and the unfolded state. A three-state model is therefore used to interpolate the thermal denaturation data. Our analysis explains how the stabilization of the intermediate conformation enhances the entropic contribution to unfolding, and thus decreases the unfolding temperature, while, at the same time, TFE enhances the conformational stability of the native fold at room temperature. Eventually, we challenged the ability of these intermediate structures to form supramolecular aggregates by heating experiments at different TFE concentrations.



## INTRODUCTION

Proteins accomplish their function when correctly folded in their native conformation. In turn, the native fold is due to a complex set of interactions, involving the residues of the polypeptide chain as well as the thermodynamic and environmental conditions of the protein solution.<sup>1</sup> This scenario is enriched by the observation that proteins are marginally stable,<sup>2</sup> and mostly thermally unstable, both upon heating and upon cooling.<sup>3</sup> The existence of partially folded protein conformations, intermediate between the native structure and the unfolded chain, is particularly important for the study of protein folding and stability.<sup>4</sup> Indeed, it is now well accepted that protein folding is not a barely stochastic process, but it follows a precise sequence of intermediate states through a decrease of the free energy.<sup>5</sup> The study of these states is very difficult because of their intrinsic short lifetime and low stability. In most cases, only the unfolded and the native state are well populated, and thus the protein folding is experimentally seen as a cooperative two state transition, with significant exceptions.<sup>6</sup>

Specific cosolutes, as alcohols, are sometimes used to alter the solution stability and to stabilize intermediate conformations. In general, alcohols affect protein refolding experiments by enhancing the folding rate,<sup>7–9</sup> or by inducing the formation of a transition intermediate.<sup>10</sup> The addition of alcohols also favors thermal unfolding by lowering the midpoint temperature of unfolding  $T_m$ .<sup>11</sup> However, the use of alcohols as denaturing agents is not straightforward. Indeed, at high alcohol concentrations the destabilizing effect on both conformational and thermodynamic

stability is prevalent, leading in some cases to the formation of elongated fibrils.<sup>12–14</sup> On the other hand, at low concentrations alcohols typically act as osmolytes,<sup>15</sup> and they may increase the solution stability by reducing protein attraction.<sup>15,16</sup> More specifically, they cause both a reduction of the bulk dielectric constant, with a subsequent increase of electrostatic repulsion, and a reduction of the entropic contribution related to the hydrophobic effect,<sup>17</sup> since their presence limit the configurational space accessible to the solvent,<sup>18</sup> likely through preferential solvation.<sup>16,19</sup>

The latter effect is correlated with a reduction of the difference in the solvent accessible area between the unfolded and the native state, which may also cause a decrease of the heat capacity difference  $\Delta C_p$ .<sup>20</sup> The decrease of  $\Delta C_p$  has been considered as the cause of the decrease of the temperature of lysozyme thermal unfolding due to alcohols.<sup>21</sup> The same effect has been also recently shown to affect protein cold denaturation.<sup>22</sup> Alternatively, the reduction of the unfolding temperature has been attributed to an increase of the unfolding entropy due to the preferential binding of alcohols to the protein molecule.<sup>23</sup>

In the present work, we study the effect of 2,2,2-trifluoroethanol (TFE) on the molecular conformation and on the thermal unfolding of hen egg-white lysozyme (HEWL), combining information coming from experiments of far-UV circular

**Received:** July 20, 2010**Revised:** February 14, 2011**Published:** March 22, 2011

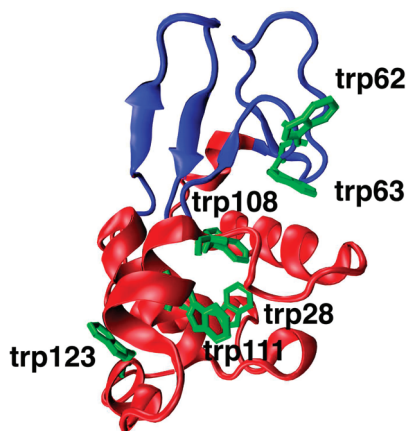


**Figure 1.** Structure of native hen egg-white lysozyme (PDB file:1AKI). The  $\alpha$  and  $\beta$ -domains are shaded in red and blue, respectively. The locations of the tryptophan side chains are indicated in green.

dichroism spectroscopy (CD), steady-state and time-resolved photoluminescence (PL) of tryptophans.

TFE is a less polar and weaker hydrogen bond donor than water, and if used as a cosolvent determines the formation of intra or intermolecular hydrogen bonds.<sup>24,25</sup> TFE may affect protein conformation either by direct mechanisms, such as the preferential binding of TFE to the helical conformers of peptides,<sup>25</sup> or preferential solvation of certain backbone groups by TFE,<sup>16,26</sup> or by indirect mechanisms, including the enhancing of the polypeptide internal H-bonding or the disruption of the water structure and the lessening of the hydrophobic effect.<sup>27</sup> For this reason TFE can modify the single protein structure, typically enhancing helical conformation;<sup>28–31</sup> it may alter the pathway of protein folding,<sup>7,8,32–34</sup> and affect proteins aggregation,<sup>16,35,36</sup> with a concentration dependent behavior.<sup>37</sup>

Lysozyme is a globular protein of 129 amino acids folded in two domains, one characterized by  $\alpha$ -helical structure ( $\alpha$ -domain) and the other mainly organized in  $\beta$ -sheets ( $\beta$ -domain) (see Figure 1). Both domains are functional for the active site cleft which is formed between them. The folding of lysozyme involves parallel alternative pathways,<sup>6</sup> and implies the formation of a transition intermediate state with a structured  $\alpha$ -domain ( $I_\alpha$ ).<sup>38,39</sup> Notwithstanding the complexity of the folding process, calorimetric thermal unfolding of hen lysozyme occurs as a single cooperative transition,<sup>40</sup> while a simple two-state unfolding does not occur in the case of equine lysozyme,<sup>41</sup> or with addition of glycerol.<sup>42</sup> Interestingly at acid pH human lysozyme exhibits an equilibrium partially folded state with conserved secondary structure features.<sup>43</sup> Calorimetric unfolding of HEWL in TFE/water mixtures has been represented as a two-state transition,<sup>44,45</sup> even if the experimental data do not exclude a more complex analysis. The addition of TFE at 25% v/v at acid pH induces a conformational transition in HEWL to a non native state, called the TFE-state,<sup>46</sup> which is reminiscent of the transition intermediate  $I_\alpha$ , since it has an increased radius of gyration,<sup>47</sup> an increased ellipticity in the  $\alpha$ -helical region,<sup>48</sup> and a protection of the  $\alpha$ -domain from H/D exchange.<sup>46</sup> A recent and thorough study has shown that TFE stabilizes the tertiary structure of lysozyme at low concentration and causes unfolding at high concentration,<sup>49</sup> even if the  $\alpha$ -helical motif may persist up to 70% TFE.<sup>28</sup>

Our PL experiments show that at the lower investigated temperatures the tryptophan emission band blue-shifts upon increasing TFE concentration, while its time-relaxation remains unchanged. At the same temperatures the CD spectra exhibit a slight change, if any. CD and PL experiments have been already done in the cited work of Povey et al.<sup>49</sup> Here, we have performed CD and static fluorescence in the same conditions, but with a sharper focus on the low TFE concentrations, and we have performed new time-resolved PL measurements, thus completing the previous findings and deepening the knowledge of the effect of low TFE concentration on lysozyme. Indeed, our results performed at room temperature point to a preferential solvation of TFE toward the protein molecule.

Moreover, upon increasing the temperature we observe a red-shift of the tryptophan emission band along with a loosening of secondary structure, as probed by CD. This monitors a thermal induced denaturation process which starts progressively at lower temperature when the TFE concentration is increased. At 20% TFE CD measurements highlight the existence of an equilibrium non-native intermediate state, characterized by a higher content of  $\alpha$ -helices. A global fit of PL and CD data with a three states model (native-intermediate-unfolded) allows us to extract the thermodynamic parameters related to the thermal denaturation process, and to draw the curve of stability of lysozyme in TFE/water mixtures, thus giving a clue to the role of alcohols in protein stabilization/destabilization. The explanation of the role of TFE in the thermal stability of lysozyme, is the main result of the present work. This was allowed by the novel finding of an equilibrium intermediate in the thermal unfolding of lysozyme in TFE/water solutions. While several kinetics intermediate state have been previously observed in refolding experiments, the identification of equilibrium intermediate states is less common. For lysozyme, the only findings we are aware of are reported in ref 23 (which dates back to 1973), and in ref 48 in the case of human lysozyme.

Moreover, inspired by the observation that the addition of TFE may cause the formation of lysozyme amyloid fibrils,<sup>12</sup> we study the dependence of lysozyme aggregation upon TFE concentration by incubation experiments at 65 °C. Macroscopic aggregation, luminescence signal of added thioflavin T and AFM imaging of incubated samples indicate that the intermediate state favors lysozyme aggregation or fibrillation.

## EXPERIMENTAL METHODS

**Sample Preparation.** All chemicals were of analytical grade. Hen egg white lysozyme (HEWL) and 2,2,2-trifluoroethanol were purchased from Sigma Chemical Co. (St. Louis, Missouri) and used without further purification. HEWL was diluted in a 50 mM phosphate buffer medium with super-Q Millipore water and a pH value of 7.0. TFE was mixed with buffer solutions to obtain the final TFE concentration. All solutions were filtered through a 0.20  $\mu$ m Millex LG syringe filter. Sample concentration was determined by UV absorption spectroscopy measurements (Shimadzu 66 UV-2401PC) using an extinction molar coefficient of 2.46  $\text{cm}^{-1} \text{mg}^{-1} \text{mL}$ . For the aggregation experiments, the samples of lysozyme (20 mg/mL) were incubated at 65 °C for 1, 3, or 20 days, and then filtered by a sterile gauze to remove the huge white lysozyme aggregates. The clean solutions so obtained were mixed with a Thioflavin T (ThT) aqueous solution to obtain a final ThT concentration of 25  $\mu\text{M}$ .

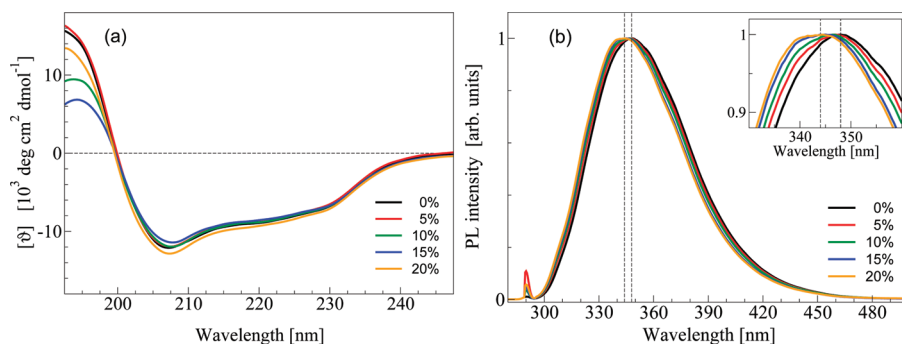


**Figure 2.** (a) CD spectra of lysozyme at 20 °C for different TFE concentrations. (b) Steady state photoluminescence spectra of lysozyme excited at 290 nm and measured at 10 °C for different TFE concentrations.

**Circular Dichroism.** The CD spectra of lysozyme at 0.2 mg/mL were recorded with a Jasco J-815 spectrometer in a quartz cell of 0.1 cm path length with the following spectral parameters: bandwidth 1 nm, scan-speed 10 nm/min, response 4 s, sensitivity 100 mdeg. Each spectrum was obtained subtracting the corresponding solvent spectrum and performing a smoothing. The temperature was set from 20 to 82 °C with 5 °C steps by a computer-controlled Peltier device, waiting 6 min for the thermalization before each measurements.

**Steady State Photoluminescence.** Steady state PL measurements were performed on lysozyme samples (0.5 mg/mL) in a Jasco FP-6500 spectrofluorimeter using a 1 cm length quartz cuvette. The spectral parameters were set as follow: excitation wavelength 290 nm for lysozyme intrinsic PL and 450 nm for Thioflavin T PL, excitation and emission bandwidth 3 nm, scan-speed 50 nm/min, response 2 s. The excitation wavelength for the intrinsic PL experiments was greater than 280 nm, corresponding to the maximum of the  ${}^1\text{L}_a - {}^1\text{L}_b$  absorption band of tryptophan, to minimize the excitation of the tyrosine residues.<sup>50</sup> The temperature of the cell holder was regulated by an external circulating bath and set from 10 to 90 °C with 5 °C steps, waiting 15 min for the thermalization. Emission spectra were fit with a sum of five Gaussian bands (with fixed centers and widths). From this set of Gaussian bands was extracted (as meaningful parameter) the first moment  $M_1$ , defined as:  $M_1 = (hc)(\int EL(E) dE)^{-1}$ , where  $L(E)$  is the normalized luminescence spectral profile at emission energy  $E$ ,  $h$  is the Planck constant, and  $c$  is the speed of light.

**Time-Resolved Photoluminescence.** Time-resolved PL measurements on lysozyme samples (0.5 mg/mL) were done at room temperature in a standard right angle geometry with a 1 cm length quartz cuvette, with the excitation of a pulsed laser tuned at 300 nm (Vibrant OPOTEK: pulselwidth of 5 ns, repetition rate of 10 Hz, energy density per pulse of  $0.10 \pm 0.02 \text{ mJ cm}^{-2}$ ). An excitation greater than 280 nm, which is the maximum of tryptophan absorption, was used to minimize the excitation of tyrosine residues and to avoid heating of the samples. The luminescence emitted by the solution was dispersed by a spectrograph (SpectraPro 2300i, PI Acton, 300 mm focal length) equipped with a 150 grooves/mm grating (blaze at 300 nm) with a spectral bandwidth of 8 nm, and detected by an air-cooled intensified charge-coupled device (CCD PIMAX, PI Acton) with a very high signal-to-noise ratio (up to  $10^4$ ) and a subnanosecond gating capability. The detection system can be electronically gated so as to acquire the emitted signal only in a given temporal window defined by its width ( $t_W$ ) and by its delay  $t$  respect to the

laser pulse.<sup>51</sup> The PL decay was followed by performing different acquisitions with the same integration time  $t_W = 0.25 \text{ ns}$  but at different delays  $t$ , going from  $-10$  to  $40 \text{ ns}$ . The laser excitation pulse was horizontally polarized and the emission signals were detected through a polarizer oriented 55 degrees from the horizontal, as required in order to avoid any polarization effect.<sup>50</sup> All the luminescence spectra were corrected for spectrograph dispersion and for instrumental response. The first moment  $M_1(t)$  of the emission bands at any delay time  $t$  was calculated as described for the steady-state PL experiments.

## RESULTS AND DISCUSSION

**Lysozyme Conformation. Circular Dichroism and Steady-State Fluorescence.** The conformational details of lysozyme at different TFE concentrations were monitored by far-UV CD and intrinsic tryptophan PL. The far-UV CD spectra of lysozyme at 20 °C as a function of TFE content, ranging from 0 to 20%, are shown in Figure 2a. It is worthwhile to note that the spectra are largely coincident, without considering the deviations of 10 and 15% TFE CD spectra in the 190 nm region. This effect could be due to an experimental artifact in a spectral region where the absorbance is high. Since far-UV CD spectra mainly results from the secondary structure features of protein molecules, we may affirm that a moderate TFE content (less than 20%) marginally affects the lysozyme secondary structure, consistent with previous findings.<sup>49</sup> The steady-state PL measurements of tryptophans in lysozyme at 10 °C as a function of TFE content, ranging from 0 to 20%, are shown in Figure 2b. These spectra elicit a consistent effect of TFE on the environment of the tryptophan residues, as observed through the blue-shift of the peak position of the tryptophan PL band from 348 nm of the pure lysozyme to 342 nm at 20% TFE (inset of Figure 2b).

**Lysozyme Solvation.** In general, tryptophan can be excited in the region of the well-known  ${}^1\text{L}_a - {}^1\text{L}_b$  absorption UV band, centered at 280 nm.<sup>50</sup> Under stationary excitation the shape and the position of the corresponding luminescence band depend on the polarity of the solvent (or in general of the environment), ranging from 355 for free tryptophan in water to about 345 for tryptophan embedded in a polypeptide chain. Indeed, the  ${}^1\text{L}_a - {}^1\text{L}_b$  states are almost isoenergetic and are characterized by different electric dipole moments. Depending on the polarity of the solvent the emission comes from the lower energy state: it is observed a structured blue-shifted band in a nonpolar environment (emission from the  ${}^1\text{L}_b$  state) or a structureless red-shifted band in a polar solvent (emission from the  ${}^1\text{L}_a$

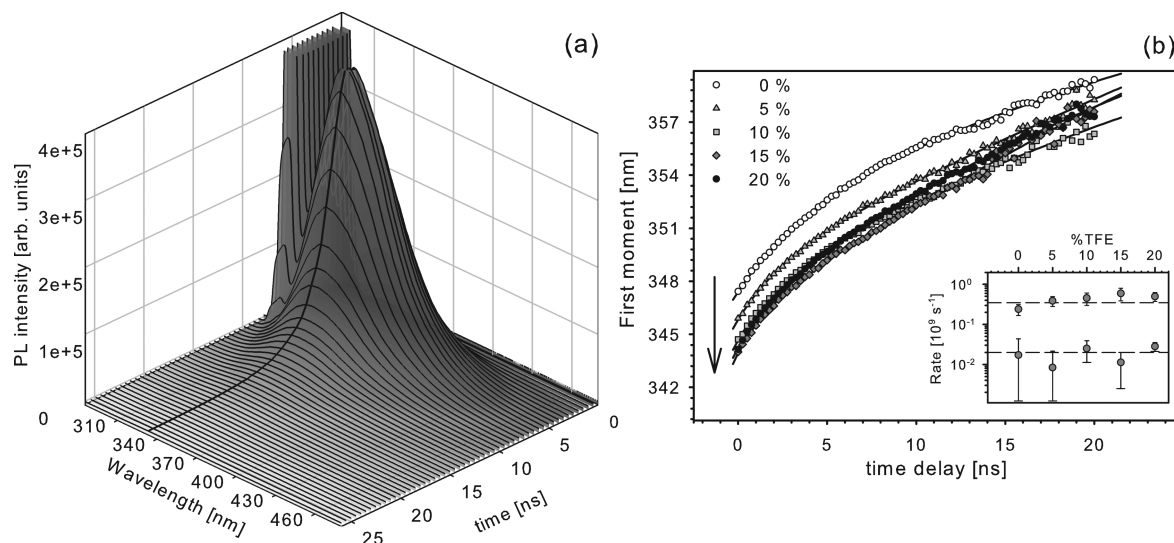


**Figure 3.** (a) Time-resolved luminescence spectra of lysozyme. The black line follows the intensity at 334 nm as an example of luminescence decay. (b) Time dependence in the nanosecond time scale of the first moment of lysozyme PL bands at increasing TFE content (following the arrow). The black lines represent the fitting with the double exponential function, as described in the text. In the inset the values of the two rates  $k'$  and  $k''$  are reported as a function of TFE content. The horizontal dashed lines are drawn as a guide to the eye.

state.<sup>50</sup> Thus, tryptophan is a very sensitive solvent polarity probe. Lysozyme has six tryptophans (see Figure 1): two located in the  $\beta$ -domain (residues 62, 63) and four in the  $\alpha$ -domain (residues 28, 108, 111, 123). The main contribution to the intrinsic tryptophan photoluminescence (>80%) is attributed to tryptophans 62 and 108,<sup>52,53</sup> the first one being completely solvent exposed and the other one being buried in the protein near the active cleft.<sup>54</sup> The remaining tryptophans are involved in electron transfer, or interaction with disulfide bond or other aminoacid quenchers and thus are less important for the global luminescence signal.<sup>52</sup> Therefore, the blue-shift observed in the present experiments can be confidently attributed to a change in the solvation properties of the exposed tryptophan 62, rather than to any other conspicuous change in the tertiary structure. More interestingly, we note that the overall change in solvent polarity due to the addition of TFE cannot explain the observed changes in the position of the PL band. Indeed, at 5% TFE the change of polarity should be too low to be felt by tryptophans to such an extent (2 nm), considering that an analogous shift (2 nm) is observed by adding up to 20% TFE. Therefore, we may argue that the tryptophan is preferentially solvated by TFE molecules that decrease the polarity of the local environment with respect to that of bulk solutions.<sup>16,49</sup>

**Lysozyme Conformation. Time-Resolved Fluorescence.** Time-resolved PL measurements of tryptophans in lysozyme at 20 °C have been performed as a function of TFE content, ranging from 0 to 20%. Figure 3a displays a representative time-resolved measurement of the PL signal of tryptophan in lysozyme excited at 300 nm at room temperature. The dynamics of tryptophan luminescence in proteins is yet not well understood, especially its intrinsic nonexponential decay. The mean lifetime of the decay from the electronic excited state of tryptophan depends critically upon the nonradiative pathways. Indeed, it may decrease from 20 ns (the pure radiative lifetime) to a few hundred of picosecond depending on the number and the effectiveness of nonradiative channels.<sup>55</sup> For instance, the solvent affects both the time features of the luminescence, by reducing the lifetime for longer emission

wavelength with the result of a dynamic red shift during the decay (spectral relaxation), and the luminescence efficiency with a temperature dependent non radiative channel.<sup>55,56</sup> Other nonradiative processes can give their contributions, as intersystem crossing, excited-state proton transfer and excited-state electron transfer. In the latter process one may include the quenching effect of the peptide bond, of the disulfide bond and of some electrophilic amino acids located near the tryptophan.<sup>56</sup> Thus, in a multityptophan protein, such as the lysozyme, contributions of each tryptophan to the spectral and temporal features of the luminescence signal can be very different. For this reason the dependence of the first moment of PL band as a function of time (in the lifetime temporal range) can be taken as a useful and compact parameter to evidence variations in the environment of all tryptophans (i.e., polarity, exposure to the solvent, interaction with other amino acids).<sup>55,57,58</sup> Figure 3b represents the time dependence of this parameter in lysozyme for the different TFE concentrations used. Two important results emerge. First, the initial values  $M_1(0)$  show a blue shift by increasing TFE concentration, accordingly to what observed in the steady-state luminescence measurements. We stress again that this should be the effect of polarity decrease caused by TFE preferential solvation shells around the exposed tryptophan 62. As a second result, the first moment of the PL spectra shows a red shift in the lifetime temporal range. The time behavior can be fit with the following double exponential function:  $M_1(t) = M_1(\infty) + M' \exp(-k't) + M'' \exp(-k''t)$ . The two characteristic rates  $k'$  and  $k''$ , shown in the panel of Figure 3b, are practically identical at all TFE concentrations. These experiments show that the solvent quenching contribution to the dynamic behavior of tryptophan emission is not altered by a TFE concentration in the range 0–20%. This consistently fosters a substantially poor influence of TFE on secondary and tertiary structure of the protein, at least for the environment of tryptophans, accompanied by the TFE preferential solvation around the protein.

**Lysozyme Thermal Denaturation. Steady State Fluorescence.** The thermal unfolding of lysozyme at different TFE concentrations was studied by intrinsic tryptophan PL and

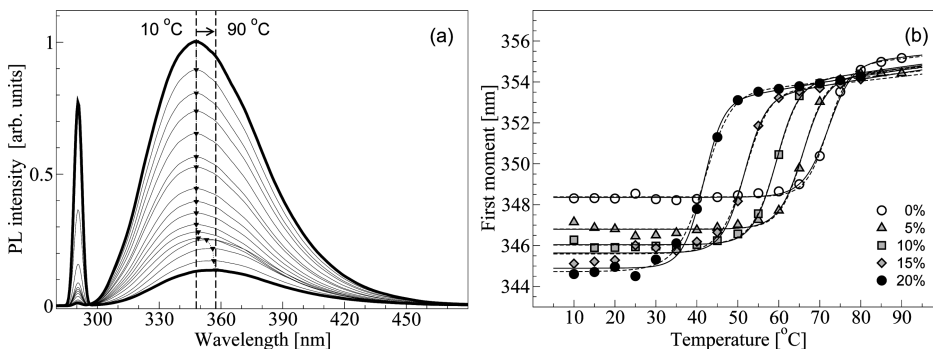


**Figure 4.** (a) Steady state PL spectra of lysozyme excited at 290 nm and measured at different temperatures. The bold black lines indicate the spectra at the lowest ( $10\text{ }^{\circ}\text{C}$ ) and the highest ( $90\text{ }^{\circ}\text{C}$ ) temperature. The black triangles indicate the position of the band peaks as a guide to the eyes. (b) Temperature dependence of the first moment of lysozyme PL band as a function of increasing TFE content. The dashed and continuous lines are the result of the fitting procedure described in the text by using a two-state or a three-state model, respectively.

far-UV CD spectra. Figure 4a displays a typical result of the thermal denaturation process measured by steady-state luminescence of tryptophan in lysozyme. At low temperatures, the spectral features of the band remain unchanged. Starting from  $65\text{ }^{\circ}\text{C}$ , the tryptophan luminescence band shows a progressive red shift which ends at  $85\text{ }^{\circ}\text{C}$ . Accordingly, the signal intensity decreases, probably due to the thermal activation of nonradiative channels, which quench the luminescence from the excited electronic state. In Figure 4a, we also note that the elastic scattering signal of exciting light at 290 nm increases as a function of temperature, indicating the growth of lysozyme aggregates caused by the prolonged thermal stress of the sample. In order to make sure that the observed spectral changes are not affected by molecular aggregation, we have performed a similar experiment using a set of fresh samples, each of them was used to measure the PL signal at selected temperatures. We observed the same spectral behavior of Figure 4a, namely the red shift and intensity decrease of the PL band, this time with a constant elastic peak. We also checked that this red shift was reversible by returning back to  $10\text{ }^{\circ}\text{C}$  and observing the initial band peak position. Similar experiments were performed for lysozyme samples with different TFE content (0, 5, 10, 15, 20%) and analogous results were obtained: a thermal red shift which starts at a temperature value which strongly depends upon the TFE concentration. Figure 4b shows the results of the first moment analysis on the steady-state PL of lysozyme. At low temperature ( $10\text{ }^{\circ}\text{C}$ ) the first moment shows a blue shift which is stronger for high TFE content, as already reported.<sup>49</sup> Notwithstanding the TFE-induced blue shift, the PL first moment clearly shows a sigmoidal red shift as a function of temperature, with a transition temperature which decreases progressively by increasing TFE concentration. At high temperature, that is at the end of the transition, the first moment remains slightly blue-shifted as a function of increasing alcohol content, indicating that the preferential solvation of TFE molecules is maintained.

**A Cooperative Conformational Transition.** We identify in this sigmoidal red-shift a cooperative conformational transition likely due to the aperture of the cleft between the  $\alpha$  and the  $\beta$  domains and the consequent exposure to the solvent of the buried tryptophan 108 (see Figure 1). This is in keeping with the lessening of hydrophobic effect due to the reduced polarity of trifluoroethanol–water mixture.<sup>18</sup> Also, the transition temperatures are in good agreement with the values related to thermal

unfolding, already found by calorimetric experiments.<sup>40,44</sup> The fluorescence signals  $M_1(T)$ , as a function of temperature  $T$ , can be fit by a two-state model, describing the unfolding as a single transition between a native (N) and an unfolded (U) state:

$$M_1(T) = (A_N + S_N T)f_N(T) + (A_U + S_U T)f_U(T) \quad (1)$$

where  $A_N$  ( $A_U$ ) and  $S_N$  ( $S_U$ ) are the intercepts and the slopes of the optical signals of the native (denatured) states, and  $f_N$  and  $f_U$  are the fractions of the population of the native and unfolded state, respectively.<sup>59</sup> Note that in the present case we can confidently set  $S_N = 0$  and  $S_U = 0.023\text{ nm K}^{-1}$ . The fraction of each state depends upon the total unfolding free energy  $\Delta G_{NU}$ :  $f_N = [1 + \exp(-\Delta G_{NU}/(k_B T))]^{-1}$ ,  $f_D = 1 - f_N$ , where  $k_B$  is the Boltzmann constant. The free energy change between two states  $i$  and  $j$  is given by the modified Gibbs–Helmholtz equation:<sup>60</sup>

$$\Delta G_{ij} = \Delta H_{ij} + \Delta C_{p,ij}(T - T_{ij}) - T[\Delta H_{ij}/T_{ij} + \Delta C_{p,ij} \ln(T/T_{ij})] \quad (2)$$

where  $T_{ij}$  is the midpoint temperature,  $\Delta H_{ij}$  is the van't Hoff enthalpy at  $T_{ij}$ , and  $\Delta C_{ij}$  is the difference in the heat capacity between the two states. Lysozyme in aqueous solution has a difference of  $6.5\text{ kJ mol}^{-1}\text{ K}^{-1}$  in heat capacity between the native and the unfolded state, slightly decreasing at moderate alcohol concentrations.<sup>21</sup> We fit the data of Figure 4b by using expressions 1 and 2 with the constraint of  $\Delta C_{NU} \leq 6.5\text{ kJ mol}^{-1}\text{ K}^{-1}$  (dashed lines in Figure 4). We obtained  $\Delta H_{NU}$  values of  $378, 347, 312, 290, 247\text{ kJ mol}^{-1}$ , and  $T_{NU}$  values of  $72, 66, 59, 52, 42\text{ }^{\circ}\text{C}$  for TFE concentrations 0, 5, 10, 15, 20% v/v, respectively. The difference in heat capacity was essentially unchanged with respect to the value of  $6.5\text{ kJ mol}^{-1}\text{ K}^{-1}$ .

An expression like eq 1 rigorously holds for the intensity of an optical signal, while in the case of the first moment of the emission spectrum it would be exact only if the quantum yields of the two states were equal. Nevertheless, it can be shown that the expression is still valid if the transition enthalpy is higher than a few  $\text{kJ mol}^{-1}$ , and the quantum yields of the two states do not differ by several orders of magnitude (see Supporting Information). Therefore, the expression is correct in all the typical cases related to unfolding or other conformational transitions.

**Lysozyme Thermal Denaturation. CD Spectra.** The thermal denaturation of lysozyme at different TFE concentration was also monitored at the level of secondary structure. In Figure 5

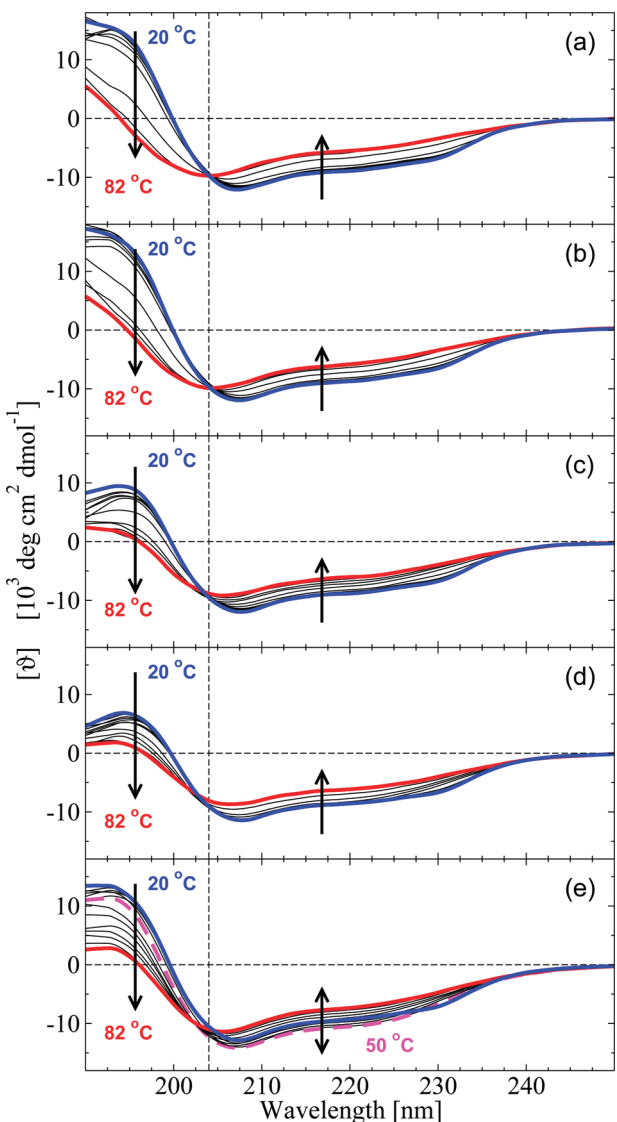


**Figure 5.** (a–e) CD spectra of lysozyme at different temperatures with 0, 5, 10, 15 and 20% of TFE, respectively. The blue and red lines indicate the spectra at the lowest (20 °C) and the highest (82 °C) temperature, respectively. The dashed magenta line in panel e indicates the spectrum at 50 °C. The vertical reference line indicates the spectral position at 204 nm.

we report the far-UV CD spectra of lysozyme at different TFE content ranging from 0 to 20% as a function of temperature, analogous to the PL experiments described above. A general trend emerges from the thermal treatment. The CD signals from the two spectral regions below and above 204 nm (vertical dashed lines in Figure 5) show a correlate decrease in absolute intensity as a function of temperature, forming indeed a quite perfect isodichroic point, which suggests a cooperative two state transition. The identification of this isodichroic point, however, fails more and more when the TFE content is increased, due to a smearing of the spectra intersections. At 20% TFE the situation is quite different. In the spectral zone between 204 and 222 nm the ellipticity increases until a negative maximum is reached at 50 °C (dashed spectrum in Figure 5e). At higher temperatures the above-described trend overwhelms this new effect causing a decrease of the absolute

intensity of the CD signal. At 20% TFE the isodichroic point is lost likely due to the interplay between these two different changes.

*An Intermediate Conformation.* The features of CD spectra in Figure 5 can be summed up by plotting the CD signal at selected wavelengths as a function of temperature (Figure 6). The two-state transition, implied by the existence of an isodichroic point, is pointed out by the temperature profile of the CD signals at 231 and 196 nm (Figure 6a), which are also linearly correlated (inset of Figure 6a). The behavior of these signals is closely related to the PL signal of Figure 4, with essentially the same transition temperatures. At variance with PL results, the observed transition seems less cooperative, extending over a large temperature range, in particular for the 20% TFE measurement. This could be rationalized considering that any tryptophan is a probe of its environment and not of the overall protein conformations, at difference with the CD spectra. The lack of cooperativity, which mirrors the smearing of the isodichroic point at increasing TFE concentration, indicates also a failure of the two-state transition model. Figure 6b yield a clear evidence of the existence of a third conformational state. Indeed, the ellipticities at 209 and 222 nm, which exhibit a strong linear correlation (inset of Figure 6b), increase negatively up to a maximum value, (at about 45 °C for 20% TFE) and then decrease again. Such a behavior is clearly visible for the 20% TFE sample, but it can be recognized also for the 15% and maybe 10% TFE samples. In other words, a different behavior is clearly observed only at 20% due to the discrete TFE concentration steps of our experiments (the previous data set is at 15%) and not due to any abrupt transition occurring at 20%. It is well accepted that variations in the ellipticity at 209 and 222 nm are related to changes in the  $\alpha$ -helical structures. Therefore, in the transition for native to thermally unfolded lysozyme the TFE stabilizes a non-native state characterized by an enhanced content of helical structures (Figure 6b), and by a more conspicuous aperture of the cleft between the  $\alpha$  and the  $\beta$  lysozyme domains (Figure 4b). This non-native state is reminiscent of the intermediate state  $I_\alpha$  identified in refolding kinetics experiments of lysozyme,<sup>38,39</sup> which is also characterized by the increase of the negative CD signal at 222 nm, and by a reduced tryptophan luminescence with respect to native values. Rothwarf and Scheraga<sup>39</sup> also note that the tryptophans 62 and 108 are involved in the folding intermediate  $I_\alpha$ , contributing to a non-native tertiary interaction between the  $\alpha$  and the  $\beta$  domains. Moreover, the  $I_\alpha$  state is very stable (10 kcal mol<sup>-1</sup>) with respect to the unfolded state and its tryptophan solvent accessibility seems almost unchanged.<sup>39</sup> Interestingly, an intermediate state of lysozyme at pH 2 was stabilized by over 15% of TFE in solution and it is again characterized by a negative increasing of ellipticity at 222 nm probably related to an increase of  $\alpha$ -helices in an opener structure, which is kept compact by the four native disulfide bonds.<sup>46,47</sup> A less recent work on the thermal unfolding of lysozyme at acid pH with different amount of alcohol has shown the formation of an intermediate equilibrium state at intermediate temperature with an increased ellipticity at 233 nm, consistent with our results.<sup>23</sup>

*A Three-State Transition.* In order to take into account the existence of the intermediate structure, we fit the data of Figures 4b, 6a, and 6b with a three-state model, describing thermal unfolding as a transition from a native (N) to an unfolded (U) state through

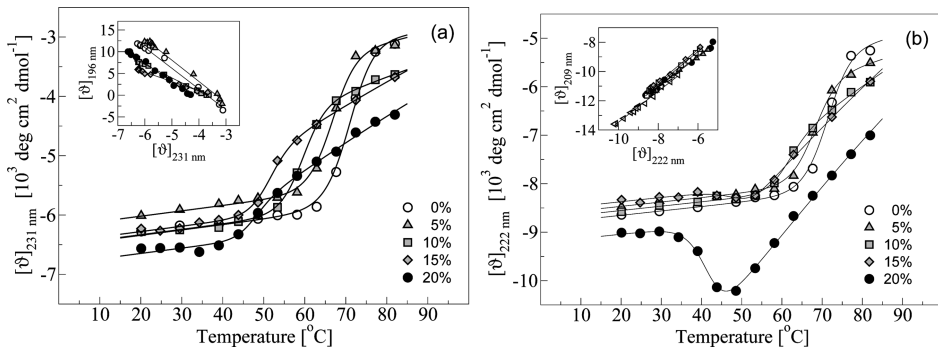


**Figure 6.** (a) Temperature dependence of the lysozyme mean residue ellipticity at 231 nm ( $[\theta]_{231\text{ nm}}$ ) at different TFE concentrations. The continuous lines are a fit to data by using a three-state model, as described in the text. Inset: Correlation between mean residue ellipticity at 231 and 196 nm; the lines are linear fit to data. (b) Temperature dependence of the lysozyme mean residue ellipticity at 222 nm ( $[\theta]_{222\text{ nm}}$ ) at different TFE concentrations. The continuous lines are a fit to data by using a three-state model, as described in the text. Inset: Correlation between mean residue ellipticity at 222 and 209 nm; the lines are linear fit to data.

an intermediate (I) state:<sup>61</sup>

$$\begin{aligned} x(T) = & [A_N^{(x)} + S^{(x)}T]f_N(T) + [A_I^{(x)} + S^{(x)}T]f_I(T) \\ & + [A_U^{(x)} + S^{(x)}T]f_U(T) \end{aligned} \quad (3)$$

where  $x(T)$  is one of the considered optical signals, namely the first moment of the tryptophan fluorescence emission band, the ellipticity at 231 and 222 nm,  $A_N^{(x)}$ ,  $A_I^{(x)}$  and  $A_U^{(x)}$  are the intercepts related to the native, intermediate and unfolded state, respectively,  $S^{(x)}$  is the slope of the optical signals, which is kept the same for the three states and is zero for the PL signal and  $9 \text{ deg cm}^2 \text{ dmol}^{-1} \text{ K}^{-1}$  for the CD signals. The fraction of the populations of the native, intermediate and denatured states are:

$$\begin{aligned} f_N &= Z^{-1} \\ f_I &= Z^{-1} \exp(-\beta\Delta G_{NI}) \\ f_U &= Z^{-1} \exp(-\beta\Delta G_{NI} - \beta\Delta G_{IU}) \end{aligned} \quad (4)$$

where  $\beta = 1/(k_B T)$ , with  $k_B$  being the Boltzmann constant, and  $Z$  is the partition function, defined so that  $f_N + f_I + f_U = 1$ . The free energy change between two states  $i$  and  $j$  is given by the modified Gibbs–Helmholtz equation, already reported in expression 2.<sup>60</sup> Expressions 2, 3 and 4 were used to interpolate the data of Figures 4b, 6a and 6b. An iterative fitting procedure was used by setting specific constraints on the parameters obtained at each iteration. In the first unconstrained fit, the difference between the heat capacities of the native and the intermediate state  $\Delta C_{p,NI}$  was driven toward high values, while the difference between the heat capacities of the intermediate and the unfolded state  $\Delta H_{IU}$  was assuming small values around zero. This was not consistent with the measurements of Velicelebi et al.<sup>21</sup> on water/alcohols solution of lysozyme. In those measurements the higher difference in heat capacity between native and unfolded lysozyme was obtained at zero alcohol concentration with a value of  $6.5 \text{ kJ mol}^{-1} \text{ K}^{-1}$ . Therefore, we constraint these quantities to the following upper values:  $\Delta C_{p,NI} = 6.5 \text{ kJ mol}^{-1} \text{ K}^{-1}$  and  $\Delta C_{p,IU} = 0$ .

We obtained  $\Delta H_{NI} = 330 \text{ kJ mol}^{-1}$ ,  $\Delta H_{IU} = 24.5 \text{ kJ mol}^{-1}$ ,  $T_{IU} = 74^\circ\text{C}$  for all the TFE concentrations, and  $T_{NI}$  values of 73, 68, 61, 52, 43 °C for TFE concentrations 0, 5, 10, 15, 20% v/v, respectively. In brief, the shift of the transition temperature at lower values is ascribed to the transition from the native to the intermediate state. Consistently, the cooperative transition

highlighted by the PL experiments is related to the formation of the intermediate state.

#### The Role of Partly Folded States in Protein Aggregation.

In order to check the thermal stability also on a longer time scale, we incubated lysozyme sample at different TFE concentration at 65 °C for three time periods: 1, 3, and 20 days. At these stages the aggregation process is essentially completed. Figure 7a shows a picture of the samples (0, 5, 10, 15, 20, 30, 50% TFE, respectively) taken after the incubation at 65 °C for 20 days. This image clearly indicates a trend of increasing turbidity from 0 to 15–20% TFE, and a residual transparency for the last two samples (30 and 50% TFE). Figure 7b displays the PL intensity of incubated samples upon addition of Thioflavin T. In the inset, the residual lysozyme concentrations are shown. For these measurements, the samples were filtered in order to remove the huge aggregates and remain with the soluble part. The ThT luminescence peak values were divided for the residual lysozyme and ThT concentrations measured by absorption spectroscopy. The results indicate an increasing of ThT luminescence, for increasing TFE content up to 15–20%, whereas for greater TFE concentration the ThT signal decreases, consistent with the visual inspection of Figure 7a. It is worth noting here that the lowest PL value is almost 3 orders of magnitude greater than the PL intensity of thioflavin in a fresh (not incubated) lysozyme sample, indicating a consistent aggregation also for the sample without TFE. Thioflavin T is a dye whose quantum yield increases upon binding to aggregated samples, and it is often proved to have a specific affinity for amyloid fibrils,<sup>62</sup> even if its emission can be enhanced by other aggregated structures.<sup>63</sup> Lysozyme has been found to form amyloid fibrils in the presence of TFE upon incubation at high temperatures.<sup>12</sup> We performed AFM experiments in order to check if the enhanced aggregation propensity at 10–15% TFE is consistent with the formation of amyloid fibrils (see Supporting Information). In most cases, the AFM images display an amorphous clustering of aggregates with a size of the orders of tens of nanometers. In one case, we observed an elongated amyloid-like structure 1 μm long and 20 nm thick. Since at 65 °C the intermediate state is more populated at a TFE concentration of 10 or 15%, these results suggest that this metastable intermediate state is also prone to favor lysozyme aggregation (and maybe fibrillation). This fact agrees with the proposed idea that non-native intermediate states, exposing their hydrophobic parts to the solvent, favor in general

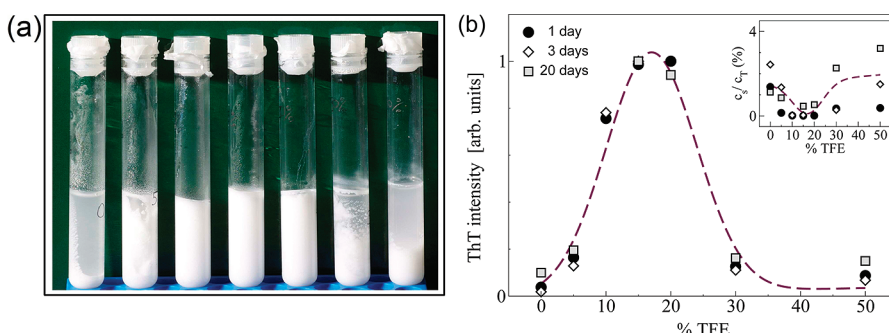


**Figure 7.** (a) Lysozyme samples after the incubation at 65 °C for 20 days: TFE concentrations (from left of right) are 0, 5, 10, 15, 20, 30, 50%. (b) Normalized Thioflavin T luminescence peak intensity measured in lysozyme samples as a function of TFE content upon incubation at 65 °C for 1 (circles), 3 (diamonds), or 20 (squares) days. The dashed line is a guide to the eyes. Lysozyme concentrations for all the samples are reported in the inset.

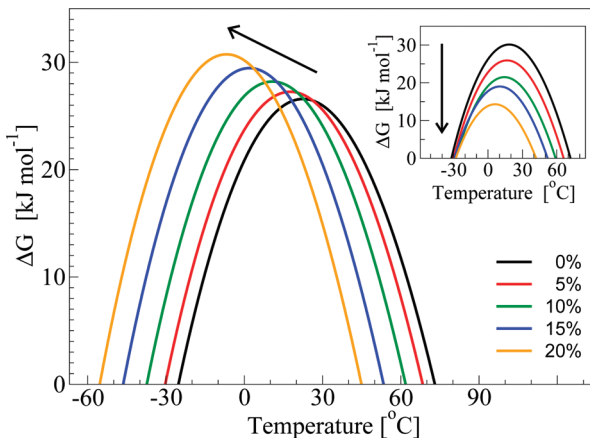


**Figure 8.** Stability curves of lysozyme at different TFE concentrations (0, 5, 10, 15, 20%) drawn by using the parameters obtained by fitting all experimental results (Figure 4b and Figure 6) with a three-state model. Inset: Stability curves of lysozyme at different TFE concentrations (0, 5, 10, 15, 20%) drawn by using the parameters obtained by fitting PL data (Figure 4b) with a two-state model.

a reciprocal interaction toward the aggregation.<sup>36</sup> In particular, for lysozyme in the intermediate  $I_\alpha$  state, the presence of a non structured  $\beta$  domain can contribute to fibril formation.

## CONCLUSIONS

**The Stability Curves of Lysozyme at Moderate TFE Concentrations.** The parameters obtained by interpolating the data of Figures 4 and 6 at different TFE concentrations were used to plot the stability curves of lysozyme, that is the curves of unfolding free-energy  $\Delta G_{NU}$ . Figure 8 displays the stability curve for the three-state model ( $\Delta G_{NU} = \Delta G_{NI} + \Delta G_{IU}$ ), where each  $\Delta_{ij}$  for  $i, j = N, I, U$  is given by expression 2. In the inset the stability curves are shown for the two-state model used in Figure 4b. Note that in both representations the temperatures at which  $\Delta G_{NU} = 0$  are identical and lowered by increasing the TFE content. When a two-state transition is considered, along with the lowering of the transition temperature, the stability curve moves down, indicating a destabilizing effect of TFE. At the opposite, the discovery of the intermediate state allows us to associate the reduction of the unfolding temperature with a shift and a slight increase of the stability curve, evidencing a stabilization of the native conformation at room temperature. This

observations are coherent with recent findings for proteins that exhibits cold denaturation at accessible temperatures.<sup>22</sup> It is worth noting that the present analysis also foresees a cold denaturation transition at low, and likely not accessible temperatures, since the free energy difference between the native and the denatured state has a convex dependence on temperature.<sup>3,64</sup>

**Conclusive Remarks.** In this work, we studied the structure and thermal stability of lysozyme at different concentrations of trifluoroethanol. At room temperature, CD spectra and the decay of the first moment in the nanosecond time scale indicate that the secondary and tertiary structure of the protein are slightly or not affected by TFE (Figures 2 and 3). The main effect is observed on the solvent exposed tryptophan 62 (Figure 1), which experiences a net change in the solvent polarity, and a consequent blue-shift of the PL emission band (Figures 2b, 3b). Such a result suggests that alcohol molecules form a preferential solvation shell around lysozyme also at small concentrations (5% TFE), consistent with previous studies.<sup>16,19</sup> Thermal denaturation of lysozyme depends upon the TFE amount, and it is accompanied by a red-shift of the PL emission band (Figure 4), associated with the solvent exposure of tryptophan 108, and by a decrease of the ellipticity on the far-UV range (Figure 5), due to the loosening of secondary structures. The addition of TFE to the system decreases progressively the transition temperature reducing the protein thermal stability. This is probably due to the lessening of hydrophobic effect because of the reduced polarity of trifluoroethanol–water mixture.<sup>18</sup> Our results revealed the existence of an intermediate non-native conformation, which is stabilized by the presence of TFE (Figures 5 and 6). Such a conformation is analogous to the intermediate  $I_\alpha$  state found in refolding experiments.<sup>38,39</sup> It is characterized by an increased amount of  $\alpha$ -helical structures (Figure 5) and by the aperture of the cleft between the  $\alpha$  and  $\beta$  domains (Figure 4). This is likely to be the cause of the enhanced propensity toward aggregation (and probably fibrillation) of such intermediate state (Figure 7). Our results are in keeping with a previous work on thermal unfolding of lysozyme at acid pH in the presence of alcohol, where an equilibrium intermediate rich in  $\alpha$ -helix has been revealed and the reduction of the unfolding temperature was attributed to an increase of the entropy of unfolding due to preferential binding to such an intermediate.<sup>23</sup> Therefore, along with the indication of a preferential solvation of lysozyme by TFE molecules, we achieved two main results: (i) we revealed the existence of an equilibrium intermediate, and (ii) we used the knowledge of the existence of such an intermediate to show the overall effect of TFE on thermal unfolding and protein stability.

The discovery of such metastable intermediate highlights the ambiguous role of alcohols, which stabilize the molecular conformation by increasing the unfolding free energy at room temperature, and at the same time foster thermal denaturation by lowering the midpoint temperature of the native to unfolded transition.

## ■ ASSOCIATED CONTENT

**§ Supporting Information.** The additional information includes a discussion related to the validity of expression 1, and the AFM experiments referred in the text, along with a picture. This material is available free of charge via the Internet at <http://pubs.acs.org>.

## ■ AUTHOR INFORMATION

### Corresponding Author

\*Telephone: +39(091)680-9305. Fax: +39(091)680-9349.  
E-mail: mauro.manno@cnr.it

### Present Addresses

<sup>§</sup>Consorzio Nazionale Interuniversitario per le Scienze Fisiche della Materia-MeSIAM, Via Archirafi 36, 90123, Palermo, Italy.

## ■ ACKNOWLEDGMENT

We thank R. Carrotta, P. L. San Biagio, A. Longo, F. M. Giordano, G. Portale for relevant discussions and collaborations, R. Noto for the assistance in drawing Figure 1. We acknowledge financial support received from the project POR Regione Sicilia - Misura 3.15 - Sottoazione C. This work was partially supported by the Italian National Research Council through the project *Intermolecular interaction in protein metastable solution*.

## ■ REFERENCES

- (1) Tanford, C. *Physical Chemistry of Macromolecules*; Wiley: New York, 1961.
- (2) Taverna, D. M.; Goldstein, R. A. *Proteins* **2002**, *46*, 105–109.
- (3) Caldarelli, G.; Rios, P. D. L. *Biol. Phys.* **2001**, *27*, 229–241.
- (4) Privalov, P. L. *J. Mol. Biol.* **1996**, *258*, 707–725.
- (5) Dobson, C. M. *Nature* **2003**, *426*, 884–890.
- (6) Radford, S. E.; Dobson, C. M.; Evans, P. A. *Nature (London)* **1992**, *358*, 302–307.
- (7) Lu, H.; Buck, M.; Radford, S. E.; Dobson, C. M. *J. Mol. Biol.* **1997**, *265*, 112–117.
- (8) Chiti, F.; Taddei, N.; Webster, P.; Hamada, D.; Fiaschi, T.; Ramponi, G.; Dobson, C. M. *Nature Struc. Biol.* **1999**, *6*, 380–387.
- (9) Lai, B.; Cao, A.; Lai, L. *Biochim. Biophys. Acta* **2000**, *1543*, 115–122.
- (10) Sasahara, K.; Demura, M.; Nitta, K. *Biochemistry* **2000**, *39*, 6475–6482.
- (11) Tanford, C. *Adv. Protein Chem.* **1970**, *24*, 1–95.
- (12) Krebs, M. R. H.; Wilkins, D. K.; Chung, E. W.; Pitkeathly, M. C.; Chamberlain, A. K.; Zurdo, J.; Robinson, C. V.; Dobson, C. M. *J. Mol. Biol.* **2000**, *300*, 541–549.
- (13) Dzwolak, W.; Jansen, R.; Smirnovas, V.; Loksztajn, A.; Porowski, S.; Winter, R. *Phys. Chem. Chem. Phys.* **2005**, *7*, 1349–1351.
- (14) Liu, W.; Prausnitz, J. M.; Blanch, H. W. *Biomacromolecules* **2004**, *105*, 1818–1823.
- (15) Javid, N.; Vogtt, K.; Krywka, C.; Tolan, M.; Winter, R. *ChemPhysChem* **2007**, *8*, 679–689.
- (16) Carrotta, R.; Manno, M.; Giordano, F. M.; Longo, A.; Portale, G.; Martorana, V.; San Biagio, P. L. *Phys. Chem. Chem. Phys.* **2009**, *11*, 4007–4018.
- (17) Cupane, A.; Giacomazza, D.; Cordone, L. *Biopolymers* **1982**, *21*, 1081–1092.
- (18) Thomas, P. D.; Dill, K. A. *Protein Sci.* **1993**, *2*, 2050–2065.
- (19) Timasheff, S. N. *Proc. Natl. Acad. Sci. U.S.A.* **2002**, *99*, 9721–9726.
- (20) Myers, J. K.; Pace, C. N.; Scholtz, J. M. *Protein Sci.* **1995**, *4*, 2138–2148.
- (21) Velicelebi, G.; Sturtevant, J. M. *Biochemistry* **1979**, *18*, 1180–1186.
- (22) Martin, S. R.; Esposito, V.; Rios, P. D. L.; Pastore, A.; Temussi, P. A. *J. Am. Chem. Soc.* **2008**, *130*, 9963–9970.
- (23) Parodi, R. M.; Bianchi, E.; Ciferri, A. *J. Biol. Chem.* **1973**, *248*, 4047–4051.
- (24) Buck, M. *Q. Rev. Biophys.* **1998**, *31*, 297–355.
- (25) Rajan, R.; Balaram, P. *Int. J. Peptide Protein Res.* **1996**, *48*, 328–336.
- (26) Roccatano, D.; Colombo, G.; Fioroni, M.; Mark, A. E. *Proc. Natl. Acad. Sci. U.S.A.* **2002**, *99*, 12179–12184.
- (27) Walgers, R.; Lee, T. C.; Cammers-Goodwin, A. *J. Am. Chem. Soc.* **1998**, *120*, 5073–5079.
- (28) Buck, M.; Schwalbe, H.; Dobson, C. M. *Biochemistry* **1995**, *34*, 13219–13232.
- (29) Shiraki, K.; Nishikawa, K.; Goto, Y. *J. Mol. Biol.* **1995**, *245*, 180–194.
- (30) Luo, Y.; Baldwin, R. L. *J. Mol. Biol.* **1998**, *279*, 49–57.
- (31) Dong, A.; Matsuura, J.; Manning, M. C.; Carpenter, J. F. *Arch. Biochem. Biophys.* **1998**, *335*, 275–281.
- (32) Hamada, D.; Chiti, F.; Guijarro, J. I.; Kataoka, M.; Taddei, N.; Dobson, C. M. *Nature Struc. Biol.* **2000**, *7*, 58–61.
- (33) Bychkova, V. E.; Dujsekina, A. E.; Klenin, S. I.; Tiktopulo, E. I.; Uversky, V. N.; Ptitsyn, O. B. *Biochemistry* **1996**, *35*, 6058–6063.
- (34) Gast, K.; Zirwer, D.; Muller-Frohne, M.; Damaschun, G. *Protein Sci.* **1999**, *8*, 625–634.
- (35) Liu, W.; Bratko, D.; Prausnitz, J. M.; Blanch, H. W. *Biophys. Chem.* **2004**, *107*, 289–298.
- (36) Grudzielanek, S.; Jansen, R.; Winter, R. *J. Mol. Biol.* **2005**, *351*, 879–894.
- (37) Hong, D.-P.; Hoshino, M.; Kuboi, R.; Goto, Y. *J. Am. Chem. Soc.* **1999**, *121*, 8427–8433.
- (38) Matagne, A.; Jamin, M.; Chung, E. W.; Robinson, C. V.; Radford, S. E.; Dobson, C. M. *J. Mol. Biol.* **2000**, *297*, 193–210.
- (39) Rothwarf, D. M.; Scheraga, H. A. *Biochemistry* **1996**, *35*, 13797–13807.
- (40) Privalov, P. L.; Khechinashvili, N. N. *J. Mol. Biol.* **1974**, *86*, 665–684.
- (41) Griko, Y. V.; Freire, E.; Privalov, G.; Van Dael, H.; Privalov, P. L. *J. Mol. Biol.* **1995**, *252*, 447–459.
- (42) Knubovets, T.; Osterhout, J. J.; Connolly, P. J.; Klibanov, A. M. *Proc. Natl. Acad. Sci. U.S.A.* **1999**, *96*, 1262–1267.
- (43) Haezebrouck, P.; Joniau, M.; Van Dael, H.; Hooke, S. D.; Woodruff, N. D.; Dobson, C. M. *J. Mol. Biol.* **1995**, *246*, 382–387.
- (44) Bhakuni, V. *Arch. Biochem. Biophys.* **1998**, *357*, 274–284.
- (45) Kundu, A.; Kishore, N. *Biophys. Chem.* **2004**, *109*, 427–442.
- (46) Buck, M.; Radford, S. E.; Dobson, C. M. *Biochemistry* **1993**, *32*, 669–678.
- (47) Hoshino, M.; Haghjira, Y.; Hamada, D.; Kataoka, M.; Goto, Y. *FEBS Lett.* **1997**, *416*, 72–76.
- (48) Galat, A. *Biochim. Biophys. Acta* **1985**, *827*, 221–227.
- (49) Povey, J.; Smales, C. M.; Hassard, S. J.; Howard, M. J. *J. Struct. Biol.* **2007**, *157*, 329–338.
- (50) Lakowicz, J. R. *Principles of Fluorescence Spectroscopy*; Kluwer Academic/Plenum Publishers: New York, 1999.
- (51) D'Amico, M.; Messina, F.; Cannas, M.; Leone, M.; Boscaino, R. *Phys. Rev. B* **2008**, *78*, 014203(1)–014203(8).
- (52) Imoto, T.; Forster, L. S.; Rupley, J. A.; Tanaka, F. *Proc. Natl. Acad. Sci. U.S.A.* **1971**, *69*, 1151–1155.
- (53) Formoso, C.; Forster, L. S. *J. Biol. Chem.* **1975**, *250*, 3738–3745.

- (54) Nishimoto, E.; Yamashita, S.; Szabo, A. G.; Imoto, T. *Biochemistry* **1998**, *37*, 5599–5607.
- (55) Engelborghs, Y. *Spectrochim. Acta, Part A* **2001**, *57*, 2255–2270.
- (56) Chen, Y.; Barkley, M. D. *Biochemistry* **1998**, *37*, 9976–9982.
- (57) Toptygin, D.; Savtchenko, R. S.; Meadow, N. D.; Brand, L. J. *Phys. Chem. B* **2001**, *105*, 2043–2055.
- (58) Otosu, T.; Nishimoto, E.; Yamashita, S. *J. Phys. Chem. A* **2009**, *113*, 2847–2853.
- (59) Masino, L.; Martin, S. R.; Bayley, P. *Protein Sci.* **2000**, *9*, 1519–1529.
- (60) Becktel, W. J.; Schellman, J. A. *Biopolymers* **1987**, *26*, 1859–1877.
- (61) Carra, J. H.; Murphy, E. C.; Privalov, P. L. *Biophys. J.* **1996**, *71*, 1994–2001.
- (62) Levine, H. *Methods Enzymol.* **1999**, *309*, 256–274.
- (63) Manno, M.; Craparo, E. F.; Podestà, A.; Bulone, D.; Carrotta, R.; Martorana, V.; Tiana, G.; San Biagio, P. L. *J. Mol. Biol.* **2007**, *366*, 258–274.
- (64) Privalov, P. L. *Crit. Rev. Biochem. Mol. Biol.* **1990**, *25*, 281–305.